Cross-Relaxation Imaging of Age-Related Changes in Myelin Mutant Shaking Pup

A. A. Samsonov[1], A. L. Alexander[2], J. V. Velikina[3], I. D. Duncan[4], and A. S. Field[1]

[1]Department of Radiology, University of Wisconsin, Madison, WI, United States, [2]Departments of Medical Physics and Psychiatry, University of Wisconsin, Madison, WI, United States, [3]Department of Medical Physics, University of Wisconsin, Madison, WI, United States, [4]School of Veterinary Medicine, University of Wisconsin, Madison, WI, United States

Introduction: Magnetization transfer imaging (MTI) is an important contrast mechanism in MRI sensitive to immobile bound protons immeasurable by conventional MRI. The traditional measure of MT effect, MT ratio (MTR), is sensitive to pathological changes of white matter (WM) in a range of diseases of central neural system [1]. Simultaneously, it is characterized by low specificity to the level of myelination and axonal loss. The low specificity and stability problems of MTR led to the development of more sophisticated MT methods based on modeling MT effect in tissues. Several investigators have adapted a two-pool model of MT for *in vivo* measurements [2-4]. The model yields physically meaningful parameters such as relative concentration of macromolecules (bound pool fraction *f*), cross-relaxation rate (*k*), and the T2 relaxation of the bound pool (*T2b*). The bound pool fraction was shown to correlate with myelin content; however, it also remains sensitive to other non-myelin components of bound pool such as axonal membranes. More complex models of MT effect were also proposed in attempt to alleviate the simplifying assumptions of the two-pool model and improve accuracy of myelin quantification [5,6]. In this abstract, we report results of studying two-pool model MT measures across ages in the *shaking* (*sh*) pup. The *sh* pup is a canine mutant with a profound paucity of myelin, without the confounding effects of axonal loss, inflammation or edema [7]. This reductionist disease model may help to elucidate specificity of individual qMT measures and disentangle the many confounding pathological changes that occur in multiple sclerosis (MS) and other WM diseases and relate them to changes in qMT measures.

Materials and Methods: Six *sh* pups and four age-matched control dogs were scanned (once or twice) at ages ranging between 3 and 21 months. The data were acquired on a 3T GE SIGNA scanner (Waukesha, Wisconsin, USA). The animal were anesthetized and imaged with a quadrature extremity coil. The protocol included collection of MT-weighted data, data for relaxation rate (R1) mapping, and data for B1 mapping. Nine MT datasets were acquired at different combinations of offset frequencies and power levels of MT saturation pulse corresponding to flip angles 500° (Δ=3, 6, 6, 9, 20 kHz) and 850° (Δ=3, 6, 9, 16 kHz) using a 3D TOF SPGR-based sequence (TR/TE=38/3.6 ms, flip=10°, 8 ms Fermi saturation pulse, image matrix 256x192, FOV=15 cm, slice thickness 1.6 mm, 60 slices). The data for R1 mapping were collected using the same sequence but without the saturation pulse at flip angles 4° and 23° (TR=21 ms, total 11 min). The data for B1 mapping were collected using multi-shot SE EPI sequence (TR/TE=10000/14.8 ms, image matrix 96x96, FOV=15 cm, slice thickness 3.2 mm, 30 slices) with two sets of flip and refocusing angles (60°/120° and 120°/240°). We used cross-relaxation imaging method [4] to estimate qMT measures. High order shimming was applied before the scans to minimize B0 inhomogeneity. Reliability of quantitative measurement based on the SPGR pulse sequence was confirmed in test-retest studies. The parameters were evaluated in regions of interest (ROIs) placed in the bilateral internal capsules to specifically assess the most compact white matter tissue.

Results and Discussion: Figure 1 shows example qMT maps both in myelinated and dysmyelinated dogs. The absence of myelin sheaths is apparently reflected by markedly decreased bound pool fraction *f* in the *sh* pup. The contrast between WM/GM is reversed on *f* maps between control and *sh* pups indicating surprisingly larger concentration of bound protons in gray matter (GM) than in severely dysmyelinated WM. These changes are consistent with our initial observations [8]. The plots in Fig. 2 show changes of qMT measures in control and mutant animals with age. The bound pool fraction progressively increases during the first months in normal animals. At the same time, no noticeable increase in *f* is present in the dysmyelinated animals. The increase of *f* during the first months probably is a manifestation of myelination present early in life of control dogs. Interestingly, *T2b* is notably decreased in *sh* pup. In control pup, the value of *T2b* increases with age in pace with myelination level revealed by age-related changes in *f*. Given different composition of bound pool in *sh* (non-myelin protons) and control (non-myelin and myelin protons) pups, these observations may serve as strong indication that both nonmyelin and myelin bound protons may be distinguished based on their *T2b*, which is a measure of mobility of protons in the bound pools. The observed increase in *R1* in control dogs with age may be biologically correlated with myelination (the longitudinal relaxation time decreases with decrease of amount of free water in intercellular space as result of myelination). Additionally, significant changes in cross-relaxation rate *k* between control and *sh* pups were observed for all ages. Insight into the pathophysiological substrates of these observations awaits forthcoming analysis of tissue from histopathology.

Conclusions: The bound pool fraction *f* provided the strongest discrimination between myelinated and dysmyelinated dogs, which supports previous observations of its high sensitivity to myelin content. Other measures (*k*, *T2b*, *R1*) were also sensitive to changes between dysmyelinated and myelinated dogs. Our results indicate that the observable qMT measures may represent a result of mixing several potentially distinguishable pools, one associated with bound protons of myelin (longer *T2b*) and the other associated with bound protons nonmyelin tissue (shorter *T2b*). Importantly, including additional bound proton pool in a MT model may potentially help distinguishing myelin from other tissues contributing to bound pool such as axonal membranes. Such extension will require inclusion of many more offset frequencies and MT pulse powers.

Acknowledgements: We acknowledge financial support of NMSS Translational Research Partnership Grant and NIH (R01 NS050466, R01NS065034).

References: [1] Morrison C, Henkelman RM, MRM 1995; 33:475. [2] Sled JG, Pike GB. MRM 2001; 46:923–931. [3] Tozer D, et al. MRM 2003; 50:83–91. [4] Yarnykh VL. MRM 47:929-939, 2002. [5] Stanisz GJ, et al. MRM 1999; 42:1128–1136. [6] Bjarnason TA, et al. MRM 2005; 54:1072–1081. [7] Duncan ID et al. Neuropathol Appl Neuobiol 1983; 9:355-368. [8] Samsonov AA, et al, ISMRM 2006, p. 3400.

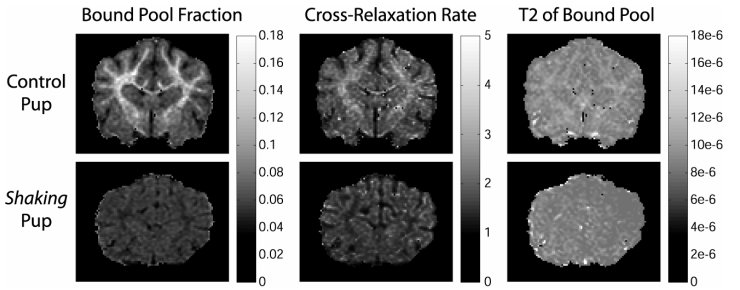

Figure 1. Representative qMT parametric maps in *sh* pup and normal dog.

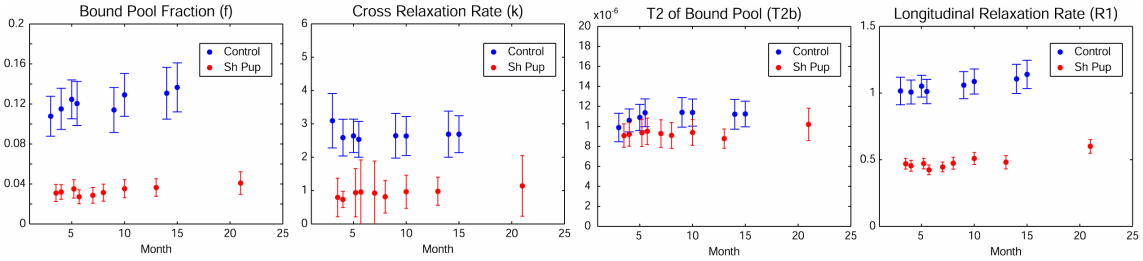

Figure 2. Plots of qMT measures across ages in white matter of *sh* pups and control dogs. The measurements were taken across 3D ROI at the bilateral internal capsules.